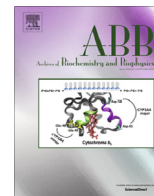




Contents lists available at ScienceDirect

Archives of Biochemistry and Biophysics

journal homepage: www.elsevier.com/locate/yabbi

Intracellular crowding effects on the self-association of the bacterial cell division protein FtsZ



Lamis Naddaf, Abdallah Sayyed-Ahmad*

Department of Physics, Birzeit University, Birzeit, Palestine

ARTICLE INFO

Article history:

Received 18 July 2014
and in revised form 21 August 2014
Available online 8 September 2014

Keywords:

Brownian dynamics
Macromolecular crowding
Protein–protein interaction
FtsZ protein

ABSTRACT

The dimerization rate of the bacterial cell division protein FtsZ is strongly affected by the intracellular crowding. Yet the complexity of the intracellular environment makes it difficult to investigate via all-atom molecular dynamics or other detailed theoretical methods. We study the crowding effect on FtsZ dimerization which is the first step of an oligomerization process that results in more elaborate supramolecular structures. In particular, we consider the effect of intracellular crowding on the reaction rates, and their dependence on the different concentrations of crowding agents. We achieved this goal by using Brownian dynamics (BD) simulation techniques and a modified post-processing approach in which we decompose the rate constant in crowded media as a product of the rate constant in the dilute solution times a factor that incorporates the crowding effect. The latter factor accounts for the diffusion reduction and crowder induced energy. In addition we include the crowding effects on water viscosity in the BD simulations of crowded media. We finally show that biomolecular crowding has a considerable effect on the FtsZ dimerization by increasing the dimerization rate constant from $2.6 \times 10^7 \text{ M}^{-1} \text{ s}^{-1}$ in the absence of crowders to $1.0 \times 10^8 \text{ M}^{-1} \text{ s}^{-1}$ at crowding level of 0.30.

© 2014 Elsevier Inc. All rights reserved.

Introduction

The bacterial cell division protein FtsZ protein plays an essential role in bacterial cell division where several FtsZ molecules bind together in the division site to form a filamentous ring that constricts when the cell divides [1]. It was shown that FtsZ proteins are capable to assemble into rings in the absence of all other *Escherichia coli* proteins [2]. Several studies experimentally investigated the effect of the crowded intracellular environment on FtsZ oligomerization. Using two inert globular proteins, cyanomethemoglobin (HbCN) and BSA, as molecular crowders with concentrations up to 150 g/L, Rivas and coworkers experimentally found that macromolecular crowding can significantly promote the dimerization of FtsZ proteins [3]. Popp and coworkers investigated crowding effect on FtsZ oligomerization. They found that above a critical crowding level (or crowder excluded volume fraction) a supra-structure of FtsZ is formed. This critical point was found to depend on the concentration of FtsZ; the lower FtsZ concentration the more crowding level is needed. They also showed that by increasing crowding level more condensed FtsZ rings were formed and the equilibrium of individual filaments was shifted to structures

composed of more than one filament [4]. González and coworkers also studied the effect of crowding on FtsZ oligomerization from the first step of FtsZ self-association passing through the cooperative formation of FtsZ filaments to the final step of assembly into ribbons. They used Ficoll and dextran as crowding agents with two concentrations of 100 g/L and 200 g/L. They found that FtsZ assembles as filaments in the absence of any crowding agent while in crowded solutions these filaments spontaneously tend to align forming dynamic ribbon polymers. The last result indicates that a non-dividing cell must have a mechanisms to stop the spontaneous assembly of the Z-ring [5].

The intracellular environment of the biological cell is heterogeneous and complex. It contains a variety of biomolecules such as lipids, sugars, nucleic acids and proteins as well as organized biomolecule arrays such as cytoplasm fibers [6]. Biochemical reactions therefore take place in an intracellular medium, which is characterized by a high total concentration of macromolecular content. Intracellular media are often called volume-occupied or crowded rather than concentrated because generally no single biomolecular species exists at high concentration, nonetheless all biomolecular species taken together occupy a significant fraction of the intracellular volume [7–11]. The volume occupancy of the macromolecular content in intracellular media typically ranges from 7% to 40%. For example, the total concentration of protein and RNA in an *E. coli*

* Corresponding author.

E-mail address: asayyeda@birzeit.edu (A. Sayyed-Ahmad).

cell is between 300 and 400 mg/ml [12,13]. Therefore to quantitatively understand biochemical processes in a real cell, it is crucial to study them *in vivo* or in an environment that effectively account for the crowding characteristics of intracellular media.

The effects of intracellular crowding on biomolecular function and interactions as well as biochemical reaction rates and equilibria are experimentally and theoretically well-established [14–22]. Crowding affects many biomolecular structures and functions related to challenging diseases. For example, it enhances the formation of the aggregates of amyloid inclusion bodies in diseases like Alzheimer [9,23]. It also plays an important role in the stabilization of G-quadruplexes that are affecting the transcription of onco-genes related to cancer [24,25]. Intracellular crowding was also established to enhance the assembly of mutated HIV-1 capsid protein [26].

Intracellular crowding was also found not only to affect solute molecule structure and function, but also as shown by Harada and coworkers [27], it impacts the water structure and dynamics by considerably increasing water viscosity and decreasing its dielectric constant. This fact is crucial as it suggests the reconsideration of previous theoretical studies of biochemical processes in crowded condition in which the effects of crowding level on water properties was not taken into account.

A typical computational method to study what happens inside the crowded environment of the cytoplasm is Brownian dynamics (BD) [28–32]. In this method, the crowding agents and the macromolecules of interest are usually represented by spheres as it is computationally infeasible to treat them at the atomistic level for most systems. Zhou and coworkers introduced the concept of *post-processing* approach to improve upon this very crude approximation. In their approach the crowding agents and the reacting proteins are studied separately at two different levels of complexity; the interacting proteins are represented at the atomic level while the crowding agents are represented by interacting spheres and studied using BD simulations. The crowding effect is then estimated by utilizing a thermodynamic cycle and method through which many insertions of the reacting proteins into the simulated crowded media are done. This approach highly reduced the computational cost required for estimating the crowding effect on biochemical reactions [33,34]. An important study that used the postprocessing approach was done by Elcock and coworkers [35]. They used a large number of proteins and other biomolecules to roughly represent the crowded cellular environment inside a real *E. coli* bacterium. They carried out all-atom rigid molecule BD simulations for the most 50 abundant proteins and RNA in the cell with their experimentally measured concentrations. These 50 macromolecules represent 85% of all cytoplasm molecules by weight, and 28% volume fraction of cytoplasm. Although Elcock and coworkers treated the crowders in atomic detail, charges were not assigned to each atom. They alternatively calculated a set of effective charges for each macromolecule [36]. This made their approach in effect a pseudo-all-atom representation. It is worth mentioning that even with the usage of effective charges, each BD simulation took a substantial time to complete.

In this study, we investigate the crowding effect on the first step of oligomerization which is FtsZ dimerization in a model *E. coli*. In particular we investigate the effect of crowding on the reaction rates, and their dependence on the different concentrations of crowding agents. We achieved this goal by using BD simulation techniques and a modified post-processing approach in which we separate the rate constant in crowded media as a product of the rate constant in the dilute solution times a factor that incorporates the crowding effect. The latter factor accounts for the diffusion reduction and crowder induced energy. In addition we include the crowding effects on water viscosity in the BD simulations of crowded media.

Methods

BD simulations of the *E. coli* model cytoplasm

The *E. coli* cytoplasm is modeled using the 50 most abundant biomolecules found in the cytoplasm of *E. coli* [35], which also have an available structure in the RCSB protein data bank. 45 of these biomolecules are found to be proteins, while the rest are RNA or RNA–protein complexes. These 50 biomolecules represent 85% of all cytoplasmic biomolecules by mass.

Each of the *E. coli* biomolecules are represented by spheres interacting by Lennard-Jones potential with its parameters were determined to reproduce the experimental value of the green fluorescent protein (GFP) translational diffusion coefficient in *E. coli* cytoplasm. For each biomolecule type, the radius of gyration R_g and the hydrodynamic radius R_H were computed using HYDROPRO software.

Fig. 1 shows the distribution of the hydrodynamic radii of biomolecules considered in our study. Notice that the most abundant molecules are these of radii between 30 Å and 40 Å. These molecules represent about half of the biomolecules considered here. Despite the significant number of biomolecules with hydrodynamic radii in the aforementioned range, one cannot conclude that the intracellular environment can be accurately approximated by crowders of uniform hydrodynamic radius. This conclusion is substantiated from the considerable fraction of biomolecules with hydrodynamic radii smaller than 30 Å as indicated by the hydrodynamic radii distribution. Although the number of biomolecules of larger radii is relatively small, their excluded volume effect is significant and cannot be ignored.

The translational diffusion coefficients D_t of all the macromolecules in infinite dilution solutions were first computed based on rigid body calculations, using the software package HYDROPRO [37], then the hydrodynamic radii were calculated according Stokes–Einstein relation.

$$D_t = \frac{k_B T}{6\pi\eta R_H} \quad (1)$$

BD simulations of the 50 macromolecule types were carried out utilizing the *bd_box* software package [28]. The integration scheme developed by Ermak and McCammon was utilized [38]. The time step was set to 2 ps. The water viscosity η was adjusted according to Harada and coworkers results [27] in which they showed that macromolecular crowding increases the water viscosity by reducing the water molecules diffusion D_{water} . Their fitted values of water translational diffusion coefficients as function of occupied volume fraction (ϕ) obey the formula

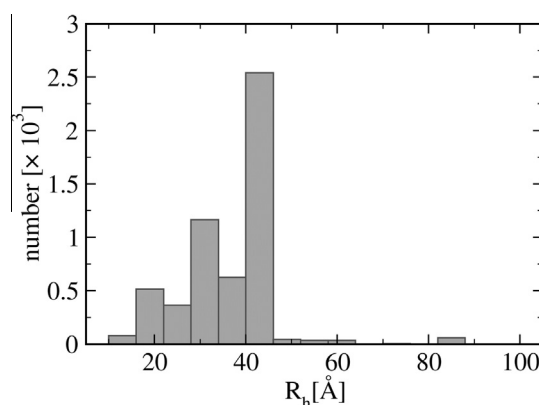


Fig. 1. Histogram of the model *E. coli* cytoplasm crowder hydrodynamic radii.

$$D_{\text{water}} = -0.569\phi + 0.308 \text{ \AA}^2/\text{ps}. \quad (2)$$

The initial position of each crowding particle is chosen randomly with the condition that it does not overlap with all other crowders. This is achieved by ordering crowder particles according to their size and then the positions of crowders are assigned in order according to their size. Following the latter algorithm is essential especially for high crowding level because if the simulation box is initially filled with the smaller crowders, then finding a position with no overlap for larger crowders will be harder or even impossible. Periodic boundary conditions were used to reduce the finite size on the diffusion coefficient calculations. The length of the simulation box in each run was adjusted according to the crowding level while keeping the number of particles constant. The total number of particles in each BD simulation was around 5000 particles and each simulation time was longer than 30 μs .

Calculation of translational diffusion coefficients

The translational diffusion coefficient (D_t) of a macromolecule is computed from its trajectory extracted from a BD simulation using the following formula [39,40]

$$D_t = \frac{1}{6} \frac{d}{dt} \lim_{t \rightarrow \infty} \langle |\vec{r}(t + \tau) - \vec{r}(t)|^2 \rangle \quad (3)$$

where $\vec{r}(t)$ is the position of the macromolecule at time t ; and τ is time interval. The averaging $\langle \rangle$ is over time and all macromolecules of a given type. Practically, the slope eventually becomes constant after a definite time and then D_t can be calculated using the formula [41]

$$D_t = \frac{1}{6} \frac{1}{(t_2 - t_1)} \langle |\vec{r}(t_2 + \tau) - \vec{r}(t_2)|^2 - |\vec{r}(t_1 + \tau) - \vec{r}(t_1)|^2 \rangle \quad (4)$$

where t_1 and t_2 are two times in the region of constant slope. It is important to account for the usage of periodic boundary conditions when calculating the translational diffusion coefficients as for example a particle that passes through a face of the cubic simulation box and enters the opposite face, seems to move about the length of the box, while actually it only moved a small distance. Depending on the direction through which the boundary crossing occurred, the length of the simulation box is added or subtracted from the position component corresponding to that direction.

Calculating crowder induced energy

The crowder induced interaction energy $\Delta\Delta G_c$ is given by the difference of the binding free energy of the two interacting proteins in the presence of crowding molecules (ΔG_{bc}) and their binding free energy in dilute solution (ΔG_b) as shown in Fig. 2.

$$\Delta\Delta G_c = \Delta G_{bc} - \Delta G_b \quad (5)$$

The latter represents the direct approach in which the crowders and the reactants are all studied together as a one large system. This approach is computationally impractical for all-atom representation of the crowders and the interacting molecules of interest since such detailed representation would contain a significant number of degrees of freedom and require long simulation times to capture the effective influence of crowders on the reactant molecules. Since resolving the short scale dynamics of the crowders are not of interest and mainly influence the reactant biomolecules through their diffusional encounters with them, we use a crude model for the crowders as spherical particles with appropriate diffusion coefficients and radii. The thermodynamic cycle shown in Fig. 2, illustrates an alternative indirect path to evaluate $\Delta\Delta G_c$ by following the vertical path where the transfer free energy from dilute to a crowded solution of each of the reactant proteins (ΔG_A and ΔG_B) and the complex (ΔG_{AB}) are utilized to evaluate $\Delta\Delta G_c$ as follows

$$\Delta\Delta G_c = \Delta G_{AB} - (\Delta G_A + \Delta G_B) \quad (6)$$

This method takes advantage of the fact that the free energy is a state function and that the crowders and the reacting biomolecules of interest can be studied separately using two different levels of modeling complexity and hence reducing the overall computational cost. The particle insertion method which was first outlined by Benjamin Widom in 1963 [42] is subsequently used to determine the transfer free energy from dilute to a crowded solution for each of the initial unbound and the final bound states of the interacting biomolecules as follows

$$\Delta G_{\text{transfer}}(\phi) = -k_B T \ln \left\langle \exp \left(-\frac{\Delta E_{in}}{k_B T} \right) \right\rangle_{\phi} \quad (7)$$

where ΔE_{in} is the interaction energy between the biomolecule of interest and the crowding agents and ϕ is the crowder occupied volume fraction. The averaging $\langle \rangle_{\phi}$ is taken over randomly selected positions and orientations and configurations of the biomolecule inserted in crowder configurations extracted from corresponding

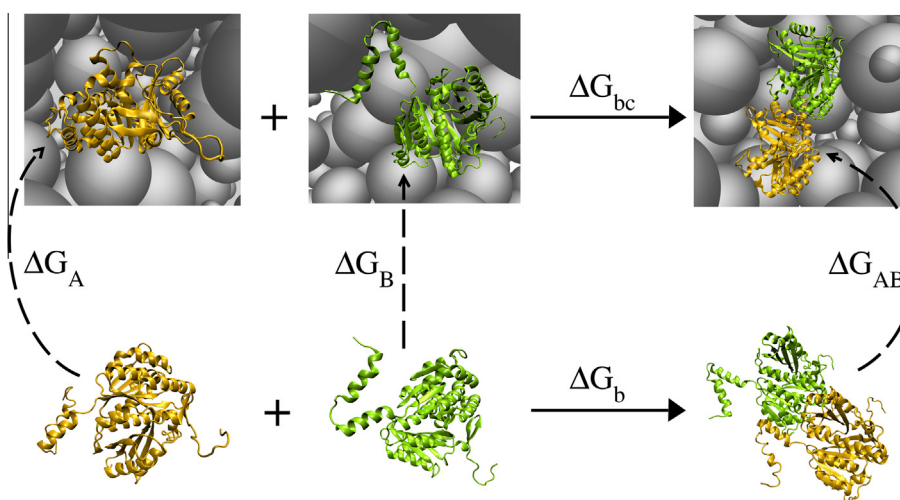


Fig. 2. Thermodynamic cycle which was used to compute the dimerization free energy of the FtsZ protein in the presence of crowding molecules.

ϕ BD simulation. Overall for the complex and each one of the interacting proteins more than 2.5 Million insertions were generated for a 500 pre-computed random orientations of 10 representative conformations extracted from an all-atom molecular dynamics (MD) simulation.

The orientations generated by rotating of a FtsZ protein and its dimer using the rotation matrix

$$\begin{bmatrix} \cos\beta\cos\gamma & \cos\gamma\sin\alpha\sin\beta - \cos\alpha\sin\gamma & \cos\alpha\cos\gamma\sin\beta + \sin\alpha\sin\gamma \\ \cos\beta\sin\gamma & \cos\alpha\cos\gamma + \sin\alpha\sin\beta\sin\gamma & -\cos\gamma\sin\alpha + \cos\alpha\sin\beta\sin\gamma \\ -\sin\beta & \cos\beta\sin\alpha & \cos\alpha\cos\beta \end{bmatrix} \quad (8)$$

where, α , β , and γ are three randomly chosen Euler angles.

For each insertion, the value of ΔE_{in} is determined to be 0 or 1 based on whether there is a steric clash between any of the proteins of interest with crowding agents. After calculating the distance between each atom of the protein and all crowding agents, the protein is said to overlap or clash with the crowders if the distance between them is less than the sum of their radii.

Rate constant in crowded media

When the range of the interaction potential between the reactant proteins is much longer than the size of the configurational space of the bound state, then the rate constant of the bimolecular association $A + B \rightleftharpoons AB$ can be written as [43]

$$K = K_0 \exp(-\Delta G/k_B T) \quad (9)$$

where K_0 is the rate constant in the absence of interaction between the two proteins, and ΔG is the binding free energy of the complex [44]. In the presence of the crowders, ΔG is the sum of the change in the electrostatic energy upon binding (ΔG_{el}) and the crowder induced interaction energy ($\Delta\Delta G_c$)

$$\Delta G = \Delta G_{el} + \Delta\Delta G_c \quad (10)$$

Now Eq. (8) can be separated into a product of the rate constant in the dilute solution times a factor that include the crowding effect

$$K = \left[K_0^{dil} \exp\left(-\frac{\Delta G_{el}}{k_B T}\right) \right] \left[\frac{K_0}{K_0^{dil}} \exp\left(-\frac{\Delta\Delta G_c}{k_B T}\right) \right] \quad (11)$$

where K_0^{dil} and K_0 are the rate constants in the absence of interactions between the two proteins in infinite dilute solution and in crowded solution, respectively. The association rate constant in infinite dilution is computed using millions of BD trajectories which were generated using the software package Browndye [45]. The rate constant was consequently computed from the ratio of the trajectories that ended up with a reaction. Each protein was treated at the all-atom level. The b radius was set to be about 100 Å as illustrated in Fig. 3. The electrostatic field around each macromolecule was computed using the nonlinear Poisson–Boltzmann solver APBS [46] with grid spacing of 0.625 Å and NaCl salt concentration of 150 mM. The PQR and APBS input files were generated using the software PDB2PQR. The protonation states of the FtsZ monomer and dimer were calculated at PH 7.6 using the empirical algorithm PropKa [47]. The temperature of all the calculations was set to 298 K.

The rate constant in absence of the interaction between the reactants is diffusion limited and is proportional to the relative diffusion D_r between them and to the sum of their radii

$$K_0 = 4\pi D_{rel}(R_1 + R_2) \quad (12)$$

Hence the ratio K_0/K_0^{dil} can be calculated by computing the ratio of the relative diffusion in crowded and infinite dilute solutions.

Completing the missing residues of FtsZ dimer structure

There are a number of flexible residues in FtsZ protein which are not resolved in any available crystal structure. The FtsZ dimer crystal structure (PDB id 1W59) which we used in this study has significant number of missing amino acids as shown in Fig. 4A. One monomer has the residues: 1, 2, 18, 19 and 355–364 missing while the other monomer has the residues 1–21 missing. To complete the missing residues, we first aligned the two monomers and the missing residues in one monomer only were duplicated in the other as shown in Fig. 4B. This step reduced the number of missing residues to four. The remaining four amino acids were generated by guessing their positions, and then equilibrated using a short molecular dynamics simulation. Fig. 4D shows the final complete structure.

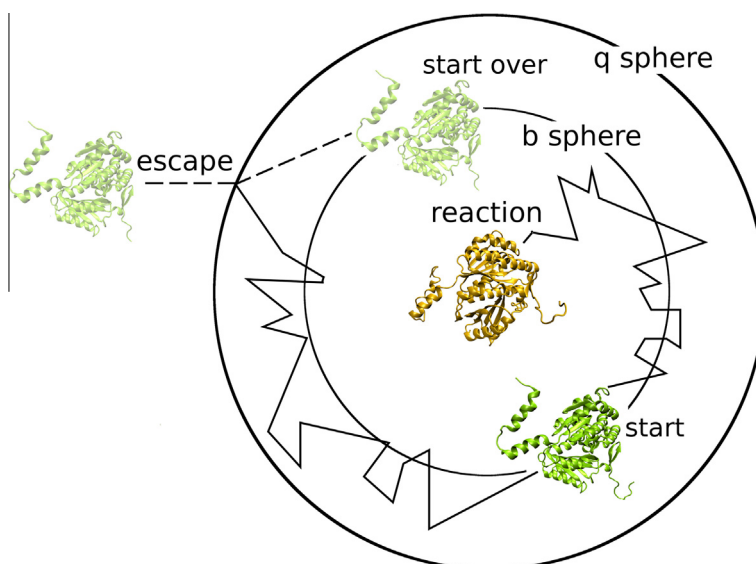


Fig. 3. Illustration of the b and q spheres utilized to compute the FtsZ dimerization rate constant in absence of crowders.

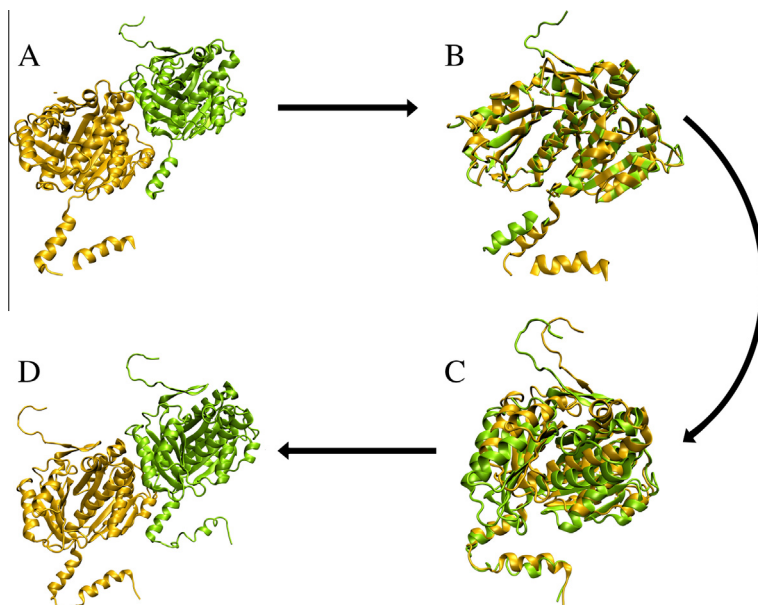


Fig. 4. The steps used for completing the FtsZ dimer crystal structure. (A) Considerable number of missing residues can be recognized by comparing the two monomers. The green dimer monomer has residues: 1–21 missing, while the yellow monomer has residues: 1, 2, 18, 19 and 355–364 missing. (B) Structure alignment of the two monomers. By doing the structure alignment the total number of missing residues was reduced to four. (C) The two aligned monomers after all of the missing residues were added and short constrained molecular dynamics simulation was done. The added residues fit the structure well. (D) The final complete dimer structure that was used as an initial structure for the unconstrained molecular dynamics simulation.

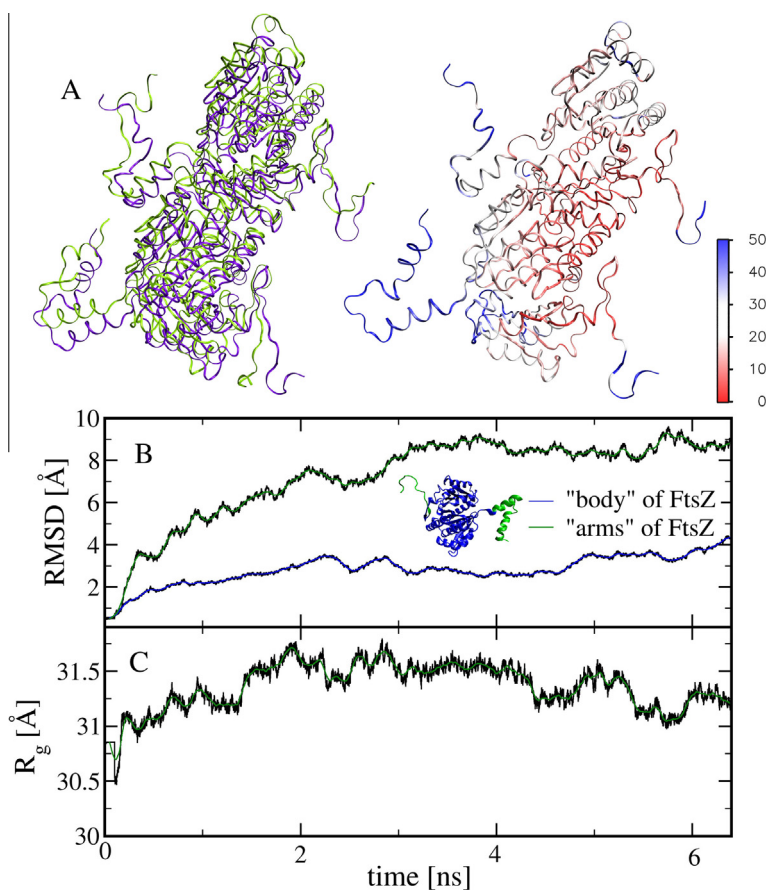


Fig. 5. (A) (Left) The initial FtsZ dimer structure (violet) and final MD simulated structure (green). (Right) The original structure colored according to the RMS deviations in Angstroms after the simulation. The RMS deviations were calculated using VMD. (B) Comparison between the RMSD of the FtsZ "arms" and the rest of the protein during the simulation. (C) The time evolution of the radius of gyration of FtsZ monomer. (For interpretation of the references to color in this figure legend, the reader is referred to the web version of this article.)

Molecular dynamics simulation FtsZ monomer and dimer

The FtsZ monomer and dimer were solvated in a box containing 25391 TIP3 waters, allowing a minimum of 10 Å distance between the edge of the box and the protein. The system was neutralized by adding 18 Na⁺ ions, and an additional 72 Na⁺ and 72 Cl⁻ ions were added to achieve a 150 mM ionic strength. Energy minimization was then carried out for 2000 steps with the protein heavy atoms fixed and for another 5000 steps with all atoms set free. During the initial 200 ps equilibration, a harmonic restraint of $k = 4 \text{ kcal mol}^{-1} \text{ \AA}^{-2}$ was applied on the C α atoms, which was then progressively reduced by $1 \text{ kcal mol}^{-1} \text{ \AA}^{-2}$ every 100 ps. All equilibration steps used a 1 fs time step, which was increased to 2 fs in the production phase with SHAKE applied to covalent bonds involving hydrogens. The temperature of the system was maintained at the physiological value of 310 K using Langevin dynamics with a damping coefficient of 2 ps^{-1} . The Nose–Hoover Langevin piston method was used to maintain constant pressure at 1 atm with a piston period of 100 fs and decay time of 50 fs. The short-range van der Waals interactions were switched off gradually between 8.5 and 10 Å with a 12 Å cutoff used for non-bonded list updates. Long-range electrostatic interactions were calculated using the Particle Mesh Ewald (PME) method. Each simulation was run for 5 ns and performed with the NAMD program [48] as well as the CHARMM27 force field [49].

The flexibility of FtsZ monomer and dimer was captured from the short MD simulation of the complete FtsZ dimer structure. Fig. 5A shows the initial and the final structures before and after the 6.5 ns simulation. Notice how the “arms” were more flexible than the rest of the dimer structure as indicated by the color code that reflects the magnitude of deviations from the initial structure.

Fig. 5B shows the RMSD of the “arms” and the rest of the protein. Notice how the RMSD of the “arms” is about three times larger. To see how the dynamics of the “arms” affected the spread of the protein which is important in the insertion calculations, we calculated the radius of gyration of the FtsZ as function of time as shown in Fig. 5C. Notice how the radius of gyration changes reached 1 Å which is a considerable change and affects the particle insertion results.

Results and discussion

Parameterizing the Lennard-Jones well depth

The translational diffusion coefficient is computed from the average of the particle squared displacements over time origins using equation 4. Fig. 6(A–D) show the displacements squared for four GFP particles with the time average is taken for each one as function of time in a medium of 30% crowding level and with

Lennard-Jones well depth of 0.1 kcal/mol. Notice that the slope of the average curve at any time represents the diffusion of this particle at that time. To compute the diffusion coefficient we must have steady slope. This steady slope is obtained by taking the average over all GFP particles. Fig. 6E shows the time average of the square of displacements for many GFP particles. The black straight line represents the average of the 40 GFP particles in the 30% crowding level medium simulation. Notice how the slope is constant and results in GFP diffusion coefficient of $1.2 \pm 0.1 \text{ \AA}^2/\text{ns}$.

The experimental values of GFP diffusion in *E. coli* was studied in several studies with the following estimates of GFP diffusion coefficients: $0.8 \pm 0.2 \text{ \AA}^2/\text{ns}$ [44], $0.9 \pm 0.2 \text{ \AA}^2/\text{ns}$ [50], $0.6 \pm 0.2 \text{ \AA}^2/\text{ns}$ [51], and $1.4 \text{ \AA}^2/\text{ns}$ [52]. The average of these values is $0.9 \pm 0.2 \text{ \AA}^2/\text{ns}$. Our result agrees with this average experimental value within experimental errors. Hence, the energy model represented by the Lennard-Jones potential with $\epsilon = 0.1 \text{ kcal mol}^{-1}$ is justified.

Effect of the heterogeneous media on diffusion coefficients calculations

Accurate estimation of the translational diffusion coefficients requires adequately calculating the time and number average such that each particle type in the system has the opportunity to sample collisions with all other particle types.

Considering a relatively short simulation or a minimal system size is insufficient for accurately calculating diffusion coefficients of our heterogeneous model cytoplasm. For example, we carried out a BD simulation of about 1000 particles for 10 μs the slope of the mean square displacements of molecules that have small number density was not constant which implies that the diffusion coefficient cannot be accurately estimated. To overcome this issue we carried out much longer BD simulations for larger system sizes at all crowding levels so that we get steadier slope.

Diffusion in *E. coli* cytoplasm

In solutions of infinite-dilution the diffusion of a spherical object is totally determined by the value of its radius according to Stokes–Einstein relation. Fig. 7 shows this relation for all crowding biomolecules in dilute solution and how the relation became in the 0.30 crowding level simulation. Notice that the diffusion in the crowded media in general seems as the diffusion occurred in a solution about 6 times more viscous. But if we look closer at the diffusion coefficients we notice that the crowding agent diffusion coefficients are not strongly correlated and there is some kind of randomness in their values. This is explained by the shape effect of the crowders. Despite our representation of them as spheres, each sphere was characterized by two different radii values. One is the radius of gyration and the other is the hydrodynamic radius. Therefore, the crowding agents do not act exactly as spheres and

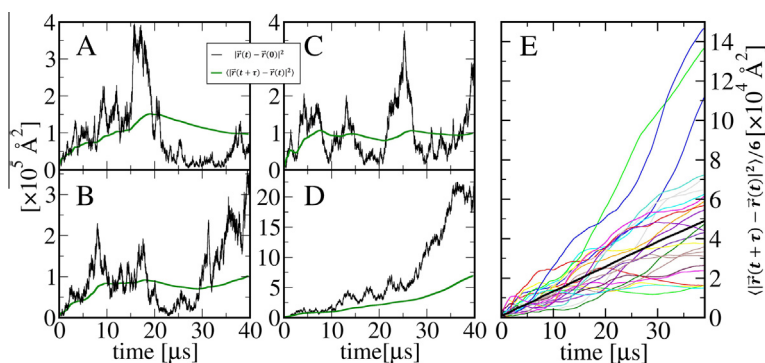


Fig. 6. (A–D) the squared displacements for four GFP particles with the time average is taken for each one as function of time. (E) the time average squared displacements for many GFP particles. The black straight line represents the average of the 40 copies of GFP in the 0.30 crowding level Brownian dynamics simulation.

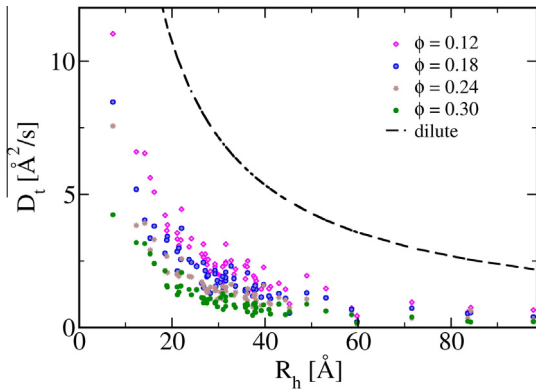


Fig. 7. Diffusion coefficient versus hydrodynamic radius in dilute and crowded media with four crowding levels of 0.12, 0.18, 0.24 and 0.30.

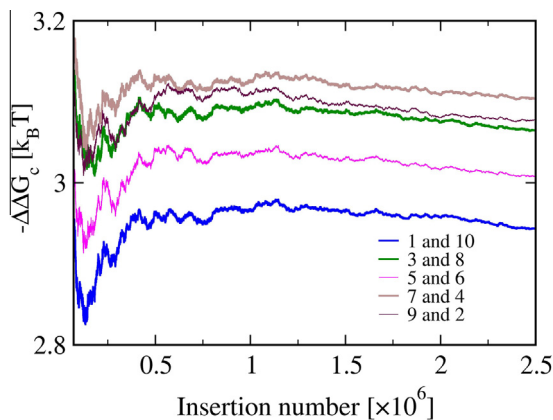


Fig. 8. $\Delta\Delta G_c$ of the five combinations of the snapshots of FtsZ MD simulation.

hence a shape effect emerges. The diffusion coefficients of all the crowding biomolecules used in this study and at the four crowding levels of 0.12, 0.18, 0.24 and 0.30 are summarized in [Table S2](#).

FtsZ dimerization crowder induced energy

10 representative frames were extracted from the 6.5 ns molecular dynamics trajectory to account for the flexibility of FtsZ

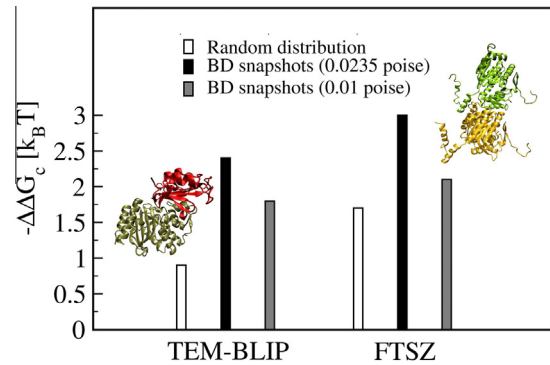


Fig. 9. The values of the crowder-induced energy for the FtsZ and the TEM-BLIP complex calculated using the *E. coli* crowded intracellular medium model considering both random crowder configuration, and configurations extracted from BD simulations that take into account the crowding effect on water at crowding level of 0.30 (0.0235 poise). The same calculations were repeated for configurations extracted from BD simulations that did not take into account the crowding effect on water (0.01 poise).

structure. The insertions were done for five different combinations of the selected 10 frames; such that half of the frames were used to get the complex structure and the other half to extract the structures of the monomers. Then combinations from the first, third, fifth, seventh, and ninth frame dimers were taken with monomers from the second, fourth, sixth, eighth, and tenth frames respectively. [Fig. 8](#) shows $\Delta\Delta G_c$ as function of insertion number for the five combinations in the 0.30 crowding level. The average of the five insertions is $-3.0 \pm 0.1 k_B T$. Notice that the values of $\Delta\Delta G_c$ converges after about million insertions, so it is safe to take a million or a million and half insertions to insure having convergent $\Delta\Delta G_c$ values.

One way to calculate $\Delta\Delta G_c$ is to do the insertion in crowded medium with the positions of the crowding biomolecules chosen randomly. This scenario resulted in a $\Delta\Delta G_c$ value of $-2.4 k_B T$ which is considerably far from the above result. This is due to the fact that the cytoplasm is not a “soup” of its constituents. These constituents are distributed in a way that is controlled by the interactions between them.

In our BD simulations we took into account the crowding effect on water, for example for the 0.30 crowded media we used the viscosity of 0.0235 poise instead of 0.01 poise. How does crowding effect on water viscosity affect the value of $\Delta\Delta G_c$? To answer this

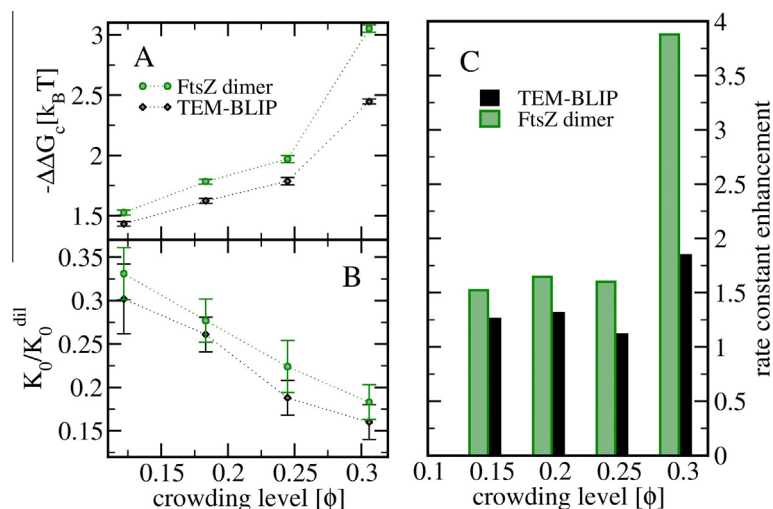


Fig. 10. (A) The values of the crowder-induced energy of the TEM-BLIP and FtsZ dimer systems versus crowding level. (B) Ratio of relative translational diffusion in dilute and crowded solutions and (C) the crowder-induced energy due to steric interactions, for the TEM-BLIP and FtsZ systems at different volume fractions.

question a BD simulation of *E. coli* crowders at occupied volume fraction of 0.30 without considering the crowding effect on water (water viscosity 0.01 poise) was carried out. The crowder induced energy was $-2.1 k_B T$ which is considerably far from our original model (see Fig. 9).

Effect of several levels of crowding on FtsZ dimerization rate constant

Crowding affects the rate of association in two different means. The first one is due to the fact that crowded environment reduces the relative diffusion between the interacting proteins which in turn reduces their association rate. The second mean is due to effect of the crowder-induced energy which increases the association rate when it has negative value. In some cases these two competitive factor cancel out and the rate constant is not affected by the crowding as was shown for the TEM-BLIP association experimentally, using inert crowding agents [53] and computationally [54]. But in some cases crowding considerably enhance the rate constant as was experimentally shown for the FtsZ protein dimerization [3]. We carried out our calculations on the TEM-BLIP association to compare with that of FtsZ dimerization. Fig. 10A shows the crowder-induced energy of the two complexes TEM-BLIP and FtsZ dimer versus crowding level. Notice that the enhancement increases by raising the crowding level. Fig. 10B shows the relative translational diffusion between the reactants in several volume fractions of the crowders divided by the relative diffusion in infinite dilution solutions. The reduction in diffusion increases by raising the crowding level. Now we have a competition. Fig. 10C shows the total crowding effect. Notice that for the two systems at all occupied volume fractions the effect is less than 2 which means that the rate constant is not significantly affected since the crowder-induced energy is cancelled by the diffusion reduction. An exception is for the FtsZ dimerization at 0.30 crowding level where the enhancement is about 4 times.

The calculated values of the association rate constants in the infinite dilution solvent and salt concentration of 150 mM for the TEM and BLIP association and dimerization of FtsZ are $(2.4 \pm 0.1) \times 10^7 \text{ M}^{-1} \text{ s}^{-1}$ and $(2.6 \pm 0.2) \times 10^7 \text{ M}^{-1} \text{ s}^{-1}$, respectively. In the 0.30 crowded media these rates became $4 \times 10^7 \text{ M}^{-1} \text{ s}^{-1}$ and $10^8 \text{ M}^{-1} \text{ s}^{-1}$, respectively.

Conclusions

Studying biochemical reaction rates under crowding conditions is essential to numerous biochemical and biotechnological problems. For example, an important aspect of developing an effective drug is increasing its association rate with its target biomolecule. This allows using smaller concentration of the drug and thereby likely reducing its side effects. One way that the intracellular crowded environment affects a rate constant is by reducing the diffusion of biomolecules due to the successive collisions with the crowder biomolecules. Other than the reduction of the reactants diffusion, crowding in general enhances the association between reactant biomolecules by increasing the opportunity for the two reactant biomolecules to be in the proper orientation for the reaction to occur.

The aim of this study was to investigate the effect of intracellular crowding on the dimerization of FtsZ protein. The usual way to study the crowding effects on biomolecular association is to first simulate the reactant proteins with the crowders, then to compute the rate constant from the reactants trajectories in the crowded media. However, this approach needs millions of reactant trajectories making it computationally expensive. To overcome the problem of high cost we adapted a “postprocessing” approach in which we simulated the interacted proteins alone and the crowd-

ers alone. This method highly decreased the computational cost since it is much faster to carry out many trajectories of the reactants separately from the crowders. In many cases these two competitive factors cancel out [53]. But in the case of FtsZ dimerization in at 0.30 crowding level, the net of these two affect reaches 4 times which match with Rivas and coworkers who found that the dimerization rate constant significantly enhanced in the presence of crowding agents [3].

Appendix A. Supplementary data

Supplementary data associated with this article can be found, in the online version, at <http://dx.doi.org/10.1016/j.abb.2014.08.016>.

References

- [1] M.A. Oliva, S.C. Cordell, J. Löwe, *Nat. Struct. Mol. Biol.* 11 (12) (2004) 1243–1250.
- [2] M. Osawa, D.E. Anderson, H.P. Erickson, *Science* 320 (5877) (2008) 792–794.
- [3] G. Rivas, J.A. Fernández, A.P. Minton, *Proc. Natl. Acad. Sci.* 98 (6) (2001) 3150–3155.
- [4] D. Popp et al., *Biopolymers* 91 (5) (2009) 340–350.
- [5] J.M. González et al., *J. Biol. Chem.* 278 (39) (2003) 37664–37671.
- [6] M.S. Cheung, D. Klimov, D. Thirumalai, *PNAS* 102 (13) (2005) 4753–4758.
- [7] A.P. Minton, *J. Biol. Chem.* 276 (14) (2001) 10577–10580.
- [8] S.B. Zimmerman, A.P. Minton, *Annu. Rev. Biophys. Biomol. Struct.* 22 (1) (1993) 27–65.
- [9] R.J. Ellis, *Trends Biochem. Sci.* 26 (10) (2001) 597–604.
- [10] D. Hall, A.P. Minton, *Biochim. Biophys. Acta (BBA) Proteins Proteomics* 1649 (2) (2003) 127–139.
- [11] R.J. Ellis, A.P. Minton, *Nature* 425 (6953) (2003) 27–28.
- [12] S.B. Zimmerman, S.O. Trach, *J. Mol. Biol.* 222 (3) (1991) 599–620.
- [13] A.B. Fulton, *Cell* 30 (2) (1982) 345–347.
- [14] A.P. Minton, *Curr. Opin. Struct. Biol.* 10 (1) (2000) 34–39.
- [15] L.D. Murphy, S.B. Zimmerman, *Biochim. Biophys. Acta (BBA) Gene Struct. Expression* 1219 (2) (1994) 277–284.
- [16] R.A. Lindner, G.B. Ralston, *Biophys. Chem.* 66 (1) (1997) 57–66.
- [17] S.B. Zimmerman, B. Harrison, *PNAS* 84 (7) (1987) 1871–1875.
- [18] Y. Qu, D.W. Bolen, *Biophys. Chem.* 101–102 (2002) 155–165.
- [19] S.B. Zimmerman, S.O. Trach, *Nucleic Acids Res.* 16 (14) (1988) 6309–6326.
- [20] A.P. Minton, *J. Cell Sci.* 119 (14) (2006) 2863–2869.
- [21] T.G. Dan, L. Sotiria, R.P. Linda, *J. Chem. Phys.* 126 (3) (2007) 034302.
- [22] S. Lampoudi, D.T. Gillespie, L.R. Petzold, *J. Comput. Phys.* 228 (10) (2009) 3656–3668.
- [23] N.A. Chebotareva, B.I. Kurganov, N.B. Livanova, *Biochemistry (Moscow)* 69 (11) (2004) 1239–1251.
- [24] S. Cogoi, L.E. Xodo, *Nucleic Acids Res.* 34 (9) (2006) 2536–2549.
- [25] K.-W. Zheng et al., *Nucleic Acids Res.* 38 (1) (2010) 327–338.
- [26] M. del Álamo, G. Rivas, M.G. Mateu, *J. Virol.* 79 (22) (2005) 14271–14281.
- [27] R. Harada, Y. Sugita, M. Feig, *J. Am. Chem. Soc.* 134 (10) (2012) 4842–4849.
- [28] M. Długosz, P. Zieliński, J. Trylska, *J. Comput. Chem.* 32 (12) (2011) 2734–2744.
- [29] J. Sun, H. Weinstein, *J. Chem. Phys.* 127 (2007) 155105.
- [30] G. Wieczorek, P. Zielenkiewicz, *Biophys. J.* 95 (11) (2008) 5030–5036.
- [31] J.S. Kim, A. Yethiraj, *Biophys. J.* 96 (4) (2009) 1333–1340.
- [32] J.S. Kim, A. Yethiraj, *Biophys. J.* 98 (6) (2010) 951–958.
- [33] Sanbo. Qin, *Biophys. J.* 97 (1) (2009) 12–19.
- [34] S. Qin et al., *J. Phys. Chem. Lett.* 1 (1) (2009) 107–110.
- [35] S.R. McGuffee, A.H. Elcock, *PLoS Comput. Biol.* 6 (3) (2010).
- [36] R.R. Gabboulline, R.C. Wade, *J. Phys. Chem.* 100 (9) (1996) 3868–3878.
- [37] J. García De La Torre, M.L. Huertas, B. Carrasco, *Biophys. J.* 78 (2000) 719–730.
- [38] D. Ermak, J. McCammon, *J. Chem. Phys.* 69 (1978) 1352.
- [39] V.A. Makarov et al., *Biophys. J.* 75 (1) (1998) 150–158.
- [40] M.P. Allen, D.J. Tildesley, *Computer Simulation of Liquids*, Oxford university press, 1989.
- [41] V. Lounnas, B. Pettitt, G. Phillips Jr, *Biophys. J.* 66 (3) (1994) 601–614.
- [42] B. Widom, *J. Chem. Phys.* 39 (2808) (1963).
- [43] S.A. Tzivia Selzer, *J. Mol. Biol.* 287 (1999) 409–419.
- [44] G. Schreiber, *Chem. Rev.* 109 (3) (2009) 839–860.
- [45] G.A. Huber, J.A. McCammon, *Comput. Phys. Commun.* 181 (11) (2010) 1896–1905.
- [46] N. Baker, M. Holst, F. Wang, *J. Comput. Chem.* 21 (15) (2000) 1343–1352.
- [47] H. Li, A.D. Robertson, J.H. Jensen, *Proteins Struct. Funct. Bioinf.* 61 (4) (2005) 704–721.
- [48] J.C. Phillips et al., *J. Comput. Chem.* 26 (16) (2005) 1781–1802.
- [49] A.D. MacKerell, N. Banavali, N. Foloppe, *Biopolymers* 56 (4) (2000) 257–265.
- [50] C.W. Mullineaux, *J. Bacteriol.* 188 (2006) 3442–3448.
- [51] M.C. Konopka, *J. Bacteriol.* 188 (2006) 6115–6123.
- [52] M.C. Konopka, *J. Bacteriol.* 191 (2009) 231–237.
- [53] Y. Phillip et al., *Biophys. J.* 103 (5) (2012) 1011–1019.
- [54] S. Qin, L. Cai, H.-X. Zhou, *Phys. Biol.* 9 (6) (2012) 066008.